Nuclear equation of state constraints from intermediate energy heavy ion collisions

Caterina Ciampi

GANIL

for the INDRA-FAZIA collaboration

Dense matter equation of state from nuclear theory and experiments
IRL - NPA workshop

FRIB, East Lansing, MI
October 28th - November 1st 2024

Isospin transport phenomena are a well known probe for studying the symmetry energy term E_{sym}

$$\mathbf{j}_n - \mathbf{j}_p \propto \frac{E_{sym}}{A}(\rho)\nabla\delta + \delta\frac{\partial \frac{E_{sym}}{A}(\rho)}{\partial\rho}\nabla\rho$$

Isospin transport phenomena

Probing the symmetry energy of the nEoS

Isospin transport phenomena are a well known probe for studying the symmetry energy term E_{sym}

diffusion

$$\mathbf{j}_n - \mathbf{j}_p \propto \frac{E_{sym}}{A}(\rho)\nabla\delta + \delta \frac{\partial \frac{E_{sym}}{A}(\rho)}{\partial \rho}\nabla\rho$$

Isospin transport phenomena

Probing the symmetry energy of the nEoS

Isospin transport phenomena are a well known probe for studying the symmetry energy term E_{sym}

diffusion

$$\mathbf{j}_n - \mathbf{j}_p \propto \frac{E_{sym}}{A}(\rho)\nabla\delta + \delta\frac{\partial\frac{E_{sym}}{A}(\rho)}{\partial\rho}\nabla\rho$$

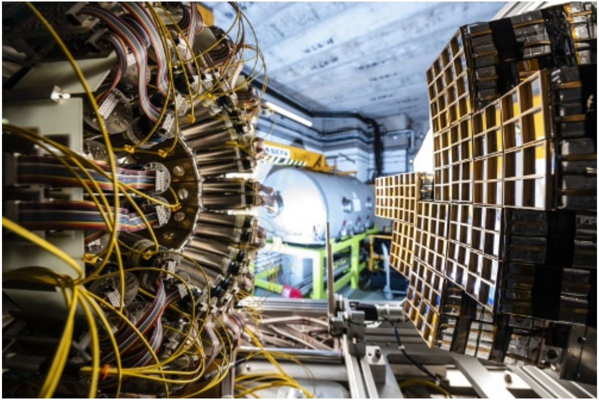

To study isospin transport, we need the **isotopic identification** (Z, A) of the produced fragments, and a **good global event reconstruction.**

INDRA FAZIA

Isospin transport phenomena
Using the INDRA-FAZIA apparatus

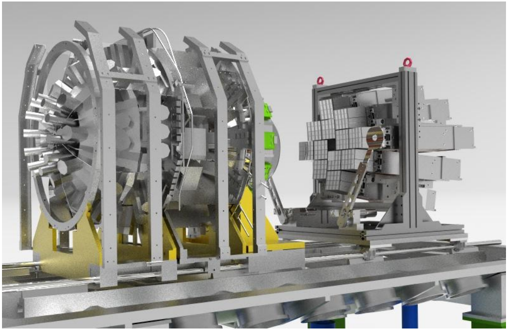

Isospin transport phenomena

Using the INDRA-FAZIA apparatus

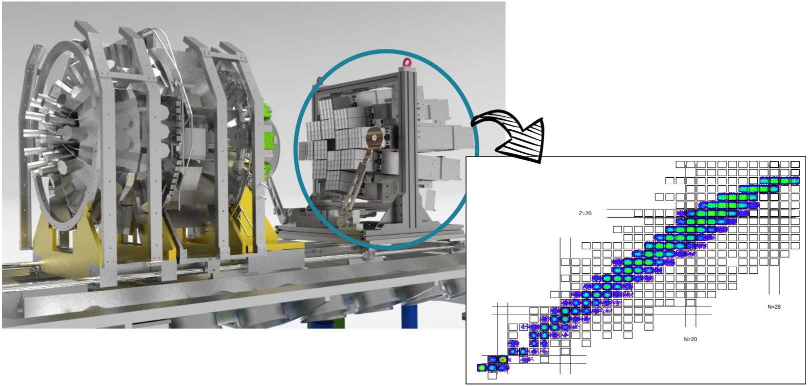

- The most forward polar angles (1.4°<θ< 12.6°) have been covered with 12 FAZIA blocks in a wall configuration at 1 m from the target.
  $\longrightarrow$ *isotopic identification of QP-like fragments*

Isospin transport phenomena

Using the INDRA-FAZIA apparatus

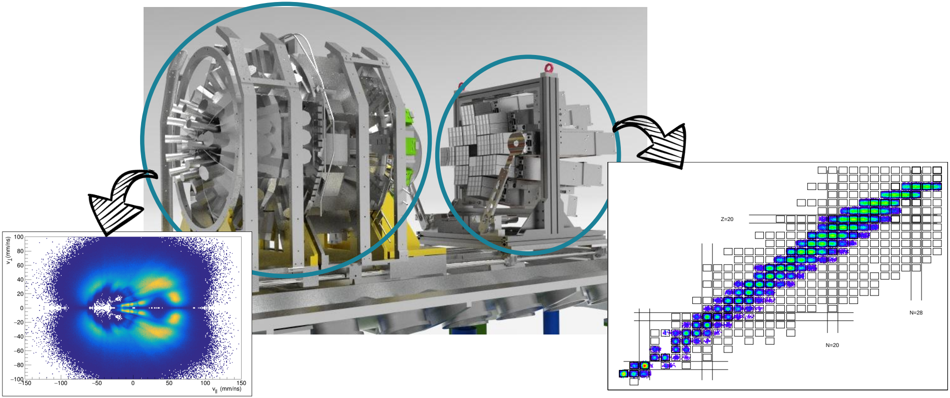

- The most forward polar angles (1.4°<θ< 12.6°) have been covered with 12 FAZIA blocks in a wall configuration at 1 m from the target.
  $\longrightarrow$ *isotopic identification of QP-like fragments*
- The remaining part of INDRA (rings 6-17) covers the polar angles between 14° and 176° ($\sim$ 80% of the 4π solid angle).
  $\longrightarrow$ *global variables for the estimation of the reaction centrality*

Isospin transport phenomena

Using the INDRA-FAZIA apparatus

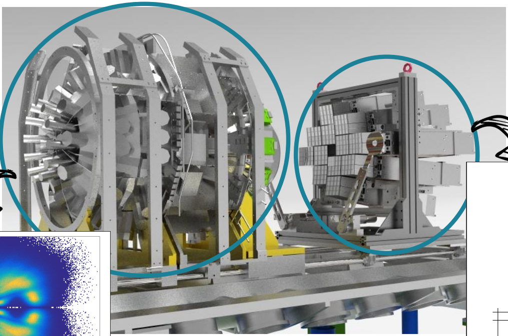

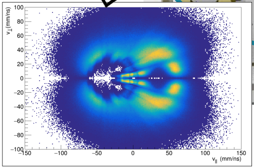

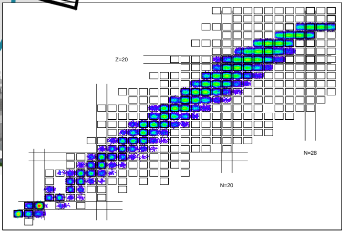

- The most forward polar angles (1.4°<θ< 12.6°) have been covered with 12 FAZIA blocks in a wall configuration at 1 m from the target.
  → *isotopic identification of QP-like fragments*
- The remaining part of INDRA (rings 6-17) covers the polar angles between 14° and 176° (∼ 80% of the 4π solid angle).
  → *global variables for the estimation of the reaction centrality*

Reaction centrality

Assessing the impact parameter in experimental data

Physical information is obtained by comparing experimental results and transport model simulations *assuming the same conditions*.

Impact parameter: experimentally, it can be only deduced from observables such as multiplicities, transverse energies, flow angle...

Reaction centrality

Assessing the impact parameter in experimental data

Physical information is obtained by comparing experimental results and transport model simulations *assuming the same conditions*.

Impact parameter: experimentally, it can be only deduced from observables such as multiplicities, transverse energies, flow angle...

All physics observables are affected by **intrinsic fluctuations** associated with the underlying processes.
Such fluctuations can limit the accuracy in treating centrality and bias the comparisons with simulated data.

L. Li et al., PRC 97,044606 (2018), G. Q. Zhang et al., PRC 84, 034612 (2011)

Reaction centrality

Assessing the impact parameter in experimental data

Physical information is obtained by comparing experimental results and transport model simulations *assuming the same conditions*.

Impact parameter: experimentally, it can be only deduced from observables such as multiplicities, transverse energies, flow angle...

All physics observables are affected by **intrinsic fluctuations** associated with the underlying processes.
Such fluctuations can limit the accuracy in treating centrality and bias the comparisons with simulated data.
L. Li et al., PRC 97,044606 (2018), G. Q. Zhang et al., PRC 84, 034612 (2011)

Different approaches for reaction centrality characterization:

- Sharp cutoff approximation C. Cavata et al., Phys. Rev. C 42, 1760 (1990)

Reaction centrality

Assessing the impact parameter in experimental data

Physical information is obtained by comparing experimental results and transport model simulations *assuming the same conditions*.

Impact parameter: experimentally, it can be only deduced from observables such as multiplicities, transverse energies, flow angle...

All physics observables are affected by **intrinsic fluctuations** associated with the underlying processes.
Such fluctuations can limit the accuracy in treating centrality and bias the comparisons with simulated data.
L. Li et al., PRC 97,044606 (2018), G. Q. Zhang et al., PRC 84, 034612 (2011)

Different approaches for reaction centrality characterization:

- Sharp cutoff approximation C. Cavata et al., Phys. Rev. C 42, 1760 (1990)
- Machine learning algorithms trained on simulations
  F. Li et al., PRC 104,034608 (2021), F. Haddad et al., PRC 55, 1371 (1997)

Reaction centrality

Assessing the impact parameter in experimental data

Physical information is obtained by comparing experimental results and transport model simulations *assuming the same conditions*.

Impact parameter: experimentally, it can be only deduced from observables such as multiplicities, transverse energies, flow angle...

All physics observables are affected by **intrinsic fluctuations** associated with the underlying processes.
Such fluctuations can limit the accuracy in treating centrality and bias the comparisons with simulated data.

L. Li et al., PRC 97,044606 (2018), G. Q. Zhang et al., PRC 84, 034612 (2011)

Different approaches for reaction centrality characterization:

- Sharp cutoff approximation C. Cavata et al., Phys. Rev. C 42, 1760 (1990)
- Machine learning algorithms trained on simulations
  F. Li et al., PRC 104,034608 (2021), F. Haddad et al., PRC 55, 1371 (1997)
- **Model-independent** method to reconstruct impact parameter distributions → includes **fluctuations**
  J. D. Frankland et al., PRC104, 034609 (2021), R. Rogly et al., PRC98, 024902 (2018)

Impact parameter reconstruction

Basic structure of the method

Centrality-related observable $X \longleftrightarrow$ deduce the correspondence with b

(see J. D. Frankland et al., PRC104, 034609 (2021), R. Rogly et al., PRC98, 024902 (2018))

$\Rightarrow$ Need to model the conditional probability distribution: $\mathbf{P(X|b)}$

Step 1

Parametrize the $\mathbf{P(X|b)}$, taking into account both the mean value and the fluctuations

Impact parameter reconstruction

Basic structure of the method

Centrality-related observable $X \longleftrightarrow$ deduce the correspondence with b

(see J. D. Frankland et al., PRC104, 034609 (2021), R. Rogly et al., PRC98, 024902 (2018))

$\Rightarrow$ Need to model the conditional probability distribution: $\mathbf{P(X|b)}$

Step 1

Parametrize the $\mathbf{P(X|b)}$, taking into account both the mean value and the fluctuations

Step 2

From the **inclusive** distribution $P(X)$, extract the $\mathbf{P(X|b)}$ parameters by fitting:

$$P(X) = \int_0^\infty P(b)\,\mathbf{P(X|b)}\,db \qquad P(b) = \frac{2\pi b}{1 + \exp\left(\frac{b-b_0}{\Delta b}\right)}$$

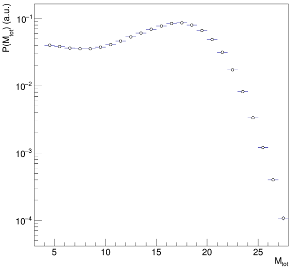

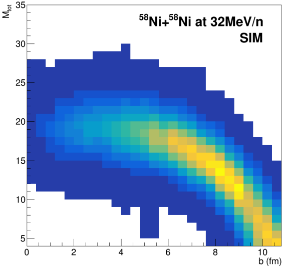

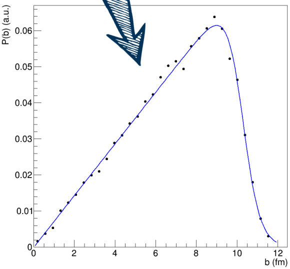

Impact parameter reconstruction

Basic structure of the method

Centrality-related observable $X \longleftrightarrow$ deduce the correspondence with b

(see J. D. Frankland et al., PRC104, 034609 (2021), R. Rogly et al., PRC98, 024902 (2018))

$\Rightarrow$ Need to model the conditional probability distribution: $\mathbf{P(X|b)}$

Step 1

Parametrize the $\mathbf{P(X|b)}$, taking into account both the mean value and the fluctuations

Step 2

From the **inclusive** distribution $P(X)$, extract the $\mathbf{P(X|b)}$ parameters by fitting:

$$P(X) = \int_0^\infty P(b)\,\mathbf{P(X|b)}\,db \qquad P(b) = \frac{2\pi b}{1 + \exp\left(\frac{b-b_0}{\Delta b}\right)}$$

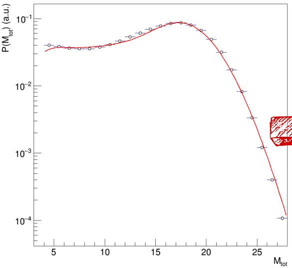

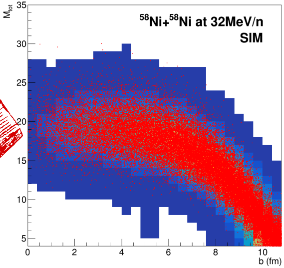

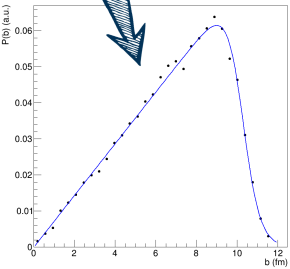

Impact parameter reconstruction

Basic structure of the method

Centrality-related observable $X \longleftrightarrow$ deduce the correspondence with b

(see J. D. Frankland et al., PRC104, 034609 (2021), R. Rogly et al., PRC98, 024902 (2018))

$\Rightarrow$ Need to model the conditional probability distribution: $\mathbf{P(X|b)}$

Step 1

Parametrize the $\mathbf{P(X|b)}$, taking into account both the mean value and the fluctuations

Step 2

From the **inclusive** distribution $P(X)$, extract the $\mathbf{P(X|b)}$ parameters by fitting:

$$P(X) = \int_0^\infty P(b)\,\mathbf{P(X|b)}\,db \qquad P(b) = \frac{2\pi b}{1 + \exp\left(\frac{b-b_0}{\Delta b}\right)}$$

Step 3

Having the $\mathbf{P(X|b)}$, for each X selection we can evaluate:

$$P(b|x_1 < X < x_2) = \frac{\int_{x_1}^{x_2} P(b,X)\,dX}{\int_{x_1}^{x_2} P(X)\,dX} = \frac{\int_{x_1}^{x_2} P(X)\,P(b|X)\,dX}{\int_{x_1}^{x_2} P(X)\,dX} = \frac{\int_{x_1}^{x_2} P(b)\,\mathbf{P(X|b)}\,dX}{\int_{x_1}^{x_2} P(X)\,dX}$$

⚠ To obtain the impact parameter distribution, it is necessary to perform the fit on the most inclusive $P(X)$ distribution, for which the $P(b)$ above can be assumed.

Here we present a combined analysis of two datasets of Ni-Ni collisions at 32 MeV/nucleon bearing complementary information:

Here we present a combined analysis of two datasets of Ni-Ni collisions at 32 MeV/nucleon bearing complementary information:

INDRA-FAZIA dataset → ^{58,64}Ni+^{58,64}Ni at 32 MeV/nucl.
Includes the information on the *isospin content of the QP remnant*.
Exp. aimed to study the **isospin diffusion mechanism** by comparing the products of the two asymmetric reactions with both the n-rich and n-deficient symmetric systems

Here we present a combined analysis of two datasets of Ni-Ni collisions at 32 MeV/nucleon bearing complementary information:

INDRA-FAZIA dataset $\rightarrow$ ^{58,64}Ni+^{58,64}Ni at 32 MeV/nucl.
Includes the information on the *isospin content of the QP remnant*.
Exp. aimed to study the **isospin diffusion mechanism** by comparing the products of the two asymmetric reactions with both the n-rich and n-deficient symmetric systems

- Trigger condition: $M_{\mathrm{FAZIA}} \geq 1$

Some events are discarded in a non-trivial way, especially for semiperipheral collisions.
The triangular $P(b)$ distribution does not well represent the experimental one.

Impact parameter reconstruction
Applying the method: overview of the INDRA and FAZIA datasets

Here we present a combined analysis of two datasets of Ni-Ni collisions at 32 MeV/nucleon bearing complementary information:

INDRA-FAZIA dataset $\rightarrow$ ^{58,64}Ni+^{58,64}Ni at 32 MeV/nucl.
Includes the information on the *isospin content of the QP remnant*.
Exp. aimed to study the **isospin diffusion mechanism** by comparing the products of the two asymmetric reactions with both the n-rich and n-deficient symmetric systems
• Trigger condition: $M_{\mathrm{FAZIA}} \geq 1$
Some events are discarded in a non-trivial way, especially for semiperipheral collisions.
The triangular $P(b)$ distribution does not well represent the experimental one.

INDRA dataset $\rightarrow$ ^{58}Ni+^{58}Ni at 32 MeV/nucl.
• Trigger condition: $M_{\mathrm{tot}} \geq 4$
Minimum bias, the $P(b)$ can be well approximated as shown before (with $\Delta b \approx 0.4$fm).
(see J. D. Frankland et al., Phys. Rev. C 104, 034609 (2021), E. Vient et al., Phys. Rev. C 98, 044612 (2018))
Suitable for the application of the *impact parameter reconstruction method*.

Procedure for the reaction in common $^{58}Ni+^{58}Ni$ at 32 MeV/nucl.:

1. Centrality estimation on "unbiased" INDRA dataset
2. Apply $X - b$ relationship to INDRA-FAZIA dataset

Impact parameter reconstruction
Implementation of the impact parameter reconstruction

Procedure for the reaction in common ^{58}Ni+^{58}Ni at 32 MeV/nucl.:

1. Centrality estimation on “unbiased” INDRA dataset
2. Apply $X - b$ relationship to INDRA-FAZIA dataset

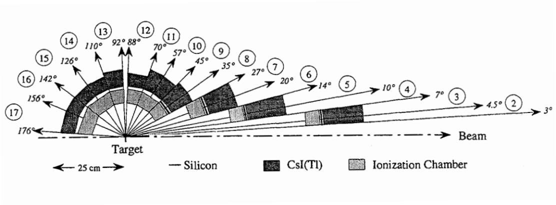

Impact parameter reconstruction

Implementation of the impact parameter reconstruction

Procedure for the reaction in common ^{58}Ni+^{58}Ni at 32 MeV/nucl.:

1. Centrality estimation on “unbiased” INDRA dataset
2. Apply $X-b$ relationship to INDRA-FAZIA dataset

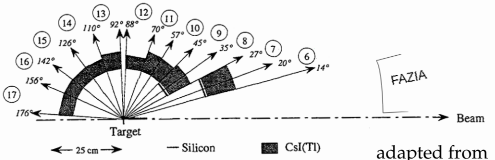

adapted from
J. Pouthas et al., NIMA 357, 418 (1995)

Impact parameter reconstruction

Implementation of the impact parameter reconstruction

Procedure for the reaction in common ^{58}Ni+^{58}Ni at 32 MeV/nucl.:

1. Centrality estimation on “unbiased” INDRA dataset
2. Apply $X - b$ relationship to INDRA-FAZIA dataset

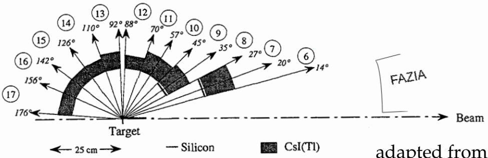

adapted from
J. Pouthas et al., NIMA 357, 418 (1995)

Centrality observable X

multiplicity M of *identified* and *unidentified* particles in INDRA rings 6 to 17.

Procedure for the reaction in common ^{58}Ni+^{58}Ni at 32 MeV/nucl.:

1. Centrality estimation on “unbiased” INDRA dataset
2. Apply $X - b$ relationship to INDRA-FAZIA dataset

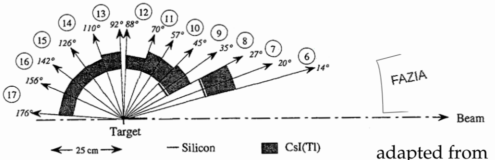

adapted from
J. Pouthas et al., NIMA 357, 418 (1995)

Centrality observable X

multiplicity M of *identified* and *unidentified* particles in INDRA rings 6 to 17.

Impact parameter reconstruction

Implementation of the impact parameter reconstruction

Procedure for the reaction in common ^{58}Ni+^{58}Ni at 32 MeV/nucl.:

1. Centrality estimation on "unbiased" INDRA dataset
2. Apply $X - b$ relationship to INDRA-FAZIA dataset

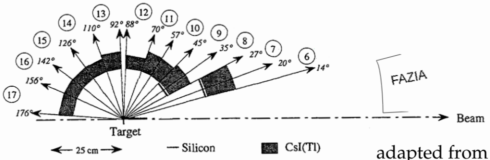

adapted from
J. Pouthas et al., NIMA 357, 418 (1995)

Centrality observable X

multiplicity M of *identified* and *unidentified* particles in INDRA rings 6 to 17.

Procedure for the reaction in common ^{58}Ni+^{58}Ni at 32 MeV/nucl.:

1. Centrality estimation on "unbiased" INDRA dataset
2. Apply $X - b$ relationship to INDRA-FAZIA dataset

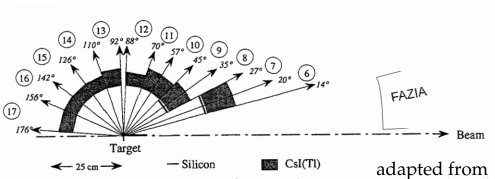

adapted from
J. Pouthas et al., NIMA 357, 418 (1995)

Centrality observable X

multiplicity M of *identified* and *unidentified* particles in INDRA rings 6 to 17.

Procedure for the other systems:

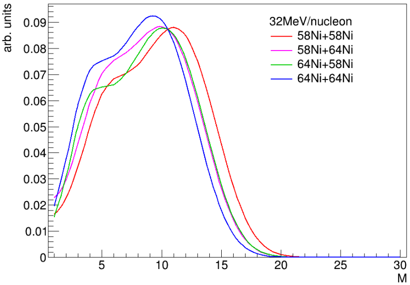

Procedure for the reaction in common ^{58}Ni+^{58}Ni at 32 MeV/nucl.:

1. Centrality estimation on "unbiased" INDRA dataset
2. Apply $X - b$ relationship to INDRA-FAZIA dataset

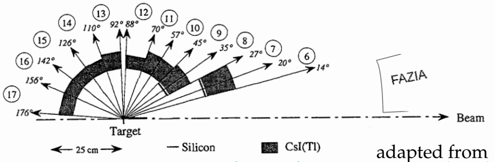

adapted from J. Pouthas et al., NIMA 357, 418 (1995)

Centrality observable X

multiplicity M of *identified* and *unidentified* particles in INDRA rings 6 to 17.

Procedure for the other systems:
→ rescale the detected multiplicity M_{sys} into a corresponding M_{resc} value for ^{58}Ni+^{58}Ni.

$$M_{resc} = \lfloor \alpha \cdot (M_{sys} + r) + \beta \rfloor$$

where $r \sim U([0,1])$ is a uniformly distributed random variable taking values in $[0,1]$.

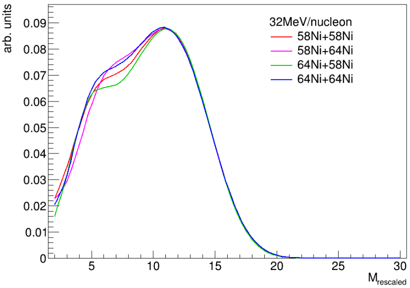

Impact parameter reconstruction

Setting the parameters for $P(b)$ model independently

To set the parameters of $P(b)$ in a model independent way:

$$P(b) = \frac{2\pi b}{1+\exp[(b-b_0)/\Delta b]}$$

- $\Delta \mathbf{b} \approx \mathbf{0.4\ fm}$ as verified in PRC 104, 034609 (2021)
- $\mathbf{b_0}$ by inverting $\sigma_R = -2\pi(\Delta b)^2 \mathrm{Li}_2\left[-\exp\left(\frac{\mathbf{b_0}}{\Delta b}\right)\right]$

Impact parameter reconstruction

Setting the parameters for $P(b)$ model independently

To set the parameters of $P(b)$ in a model independent way:

$$P(b) = \frac{2\pi b}{1+\exp[(b-b_0)/\Delta b]}$$

- $\mathbf{\Delta b} \approx \mathbf{0.4\ fm}$ as verified in PRC 104, 034609 (2021)
- $\mathbf{b_0}$ by inverting $\sigma_R = -2\pi(\Delta b)^2 \mathrm{Li}_2\left[-\exp\left(\frac{\mathbf{b_0}}{\Delta b}\right)\right]$

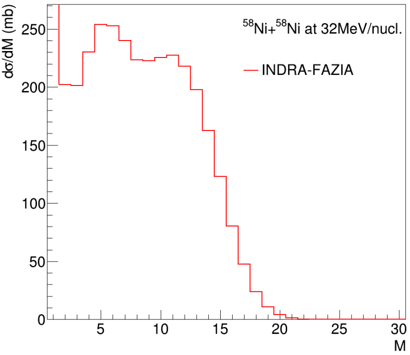

For the estimation of σ_R, and hence b_0:

- Use the elastic scattering events in the INDRA-FAZIA dataset ($M_{FAZIA} \geq 1$) as reference for cross section normalization

Impact parameter reconstruction

Setting the parameters for $P(b)$ model independently

To set the parameters of $P(b)$ in a model independent way:

$$P(b) = \frac{2\pi b}{1+\exp[(b-b_0)/\Delta b]}$$

$\Delta \mathbf{b} \approx \mathbf{0.4\ fm}$ as verified in PRC 104, 034609 (2021)

$\mathbf{b_0}$ by inverting $\sigma_R = -2\pi(\Delta b)^2 \mathrm{Li}_2\left[-\exp\left(\frac{\mathbf{b_0}}{\Delta b}\right)\right]$

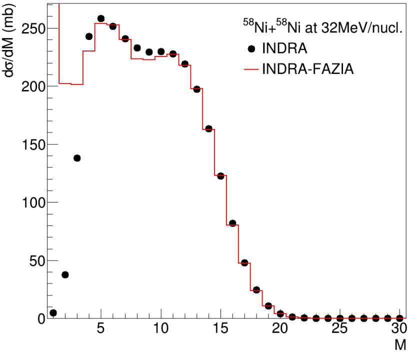

For the estimation of σ_R, and hence b_0:

- Use the elastic scattering events in the INDRA-FAZIA dataset ($M_{FAZIA} \geq 1$) as reference for cross section normalization
- Transfer the normalization to the INDRA dataset using the high multiplicity tail, after correcting for small trigger effect

To set the parameters of $P(b)$ in a model independent way:

$$P(b) = \frac{2\pi b}{1+\exp[(b-b_0)/\Delta b]}$$

Δb $\approx$ 0.4 fm as verified in PRC 104, 034609 (2021)

b_0 by inverting $\sigma_R = -2\pi(\Delta b)^2 \mathrm{Li}_2\left[-\exp\left(\frac{b_0}{\Delta b}\right)\right]$

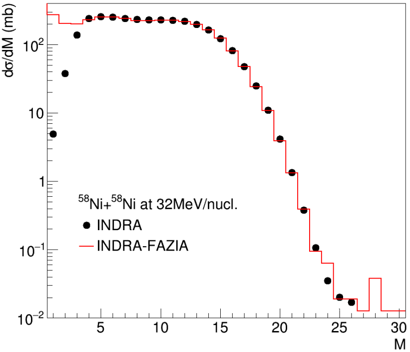

For the estimation of σ_R, and hence b_0:

- Use the elastic scattering events in the INDRA-FAZIA dataset ($M_{FAZIA} \geq 1$) as reference for cross section normalization
- Transfer the normalization to the INDRA dataset using the high multiplicity tail, after correcting for small trigger effect
- From the total reaction cross section σ_R for INDRA dataset $\Rightarrow b_0 = (9.8 \pm 0.7)$ fm

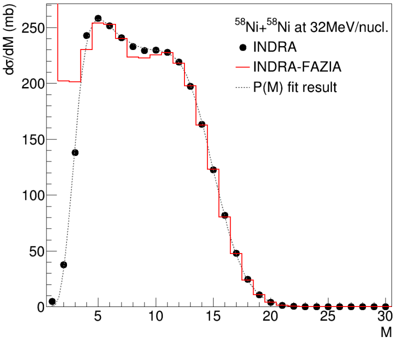

Fit result on multiplicity M of identified and unidentified particles in INDRA rings 6-17 for ^{58}Ni+^{58}Ni at 32 MeV/nucleon on INDRA dataset

Impact parameter reconstruction
Results of the method

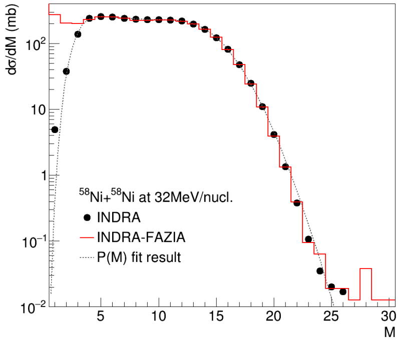

Fit result on multiplicity M of identified and unidentified particles in INDRA rings 6-17 for ^{58}Ni+^{58}Ni at 32 MeV/nucleon on INDRA dataset

Impact parameter reconstruction

Results of the method

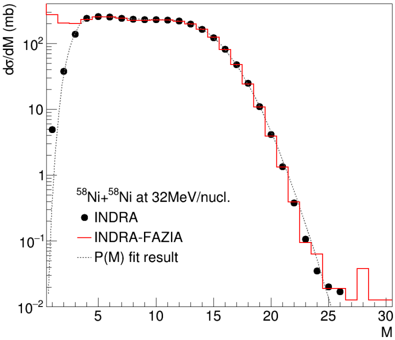

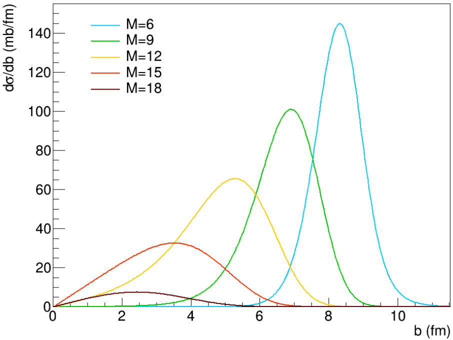

Fit result on multiplicity M of identified and unidentified particles in INDRA rings 6-17 for ^{58}Ni+^{58}Ni at 32 MeV/nucleon on INDRA dataset

→ important role of **intrinsic fluctuations**: relatively different M selections populate partly (or entirely) superimposed b intervals

In view of producing the most general result, easily comparable with theoretical prediction, we avoid a strictly exclusive analysis.

- No distinction among different output channels
- QP remnant selected as:
  1. fragment with largest Z in forward hemisphere
  2. if more than one with same Z, select largest $v_z^{c.m.}$
- Minimum size to consider a QP remnant: $Z_{QP} \geq 5$
  → include light products from very dissipative events

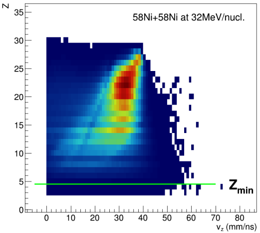

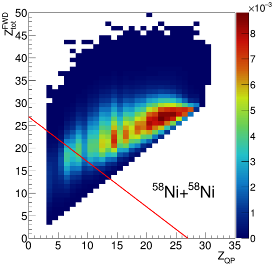

Since we are considering such light QP remnants it is necessary to carefully check the completeness of the event to exclude those in which the heaviest fragment has been lost.

- The total undetected charge in the forward hemisphere should not exceed Z_{QP}
- Accept event if $Z_{QP} \geq 28 - Z_{tot}^{FWD}$
- We verified that by removing < 13% of events, the final result becomes stable against reasonable variations of Z_{QP}^{min}

Isospin analysis

Evolution of isospin equilibration with centrality

From the distributions of (Z_{QP}, A_{QP}) vs M_{resc}, the number of counts for each produced nuclear species for each M_{resc} value is independently redistributed according to the corresponding b distribution $\Rightarrow$ take into account the fluctuations

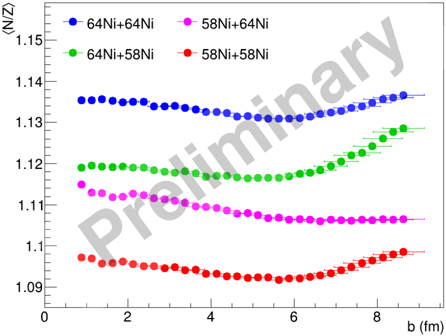

Model-independent ⟨N/Z⟩ for the QP remnant as a function of b for the four systems in the INDRA-FAZIA dataset

Clear effect of isospin equilibration down to the most central collisions:

- *peripheral*: similar result for reactions with same projectile
- *central*: ⟨N/Z⟩ depends on target, mixed systems tend to each other

The horizontal error bars are associated with the uncertainty on the estimation of b_0 in the $P(b)$ assumed for the impact parameter reconstruction method, affecting less central collisions to a greater extent.

Isospin transport ratio: can highlight the isospin diffusion effect, bypassing the effects acting similarly on the four systems (F. Rami et al., Phys. Rev. Lett. 84, 1120 (2000))

$$R(x) = \frac{2x_i - x_{AA} - x_{BB}}{x_{AA} - x_{BB}}$$

$R(x) = \pm 1 \rightarrow$ non equilibrated

$R(x_{AB}) = R(x_{BA}) \rightarrow$ full equilibration

where $A = {}^{64}$Ni, $B = {}^{58}$Ni, $i = AA, AB, BA, BB$ and x is an isospin sensitive observable.

Model-independent isospin transport ratio R(⟨N/Z⟩) for the QP remnant as a function of the impact parameter b

Regular behavior towards equilibration for increasing centralities (full equilibration is not achieved).

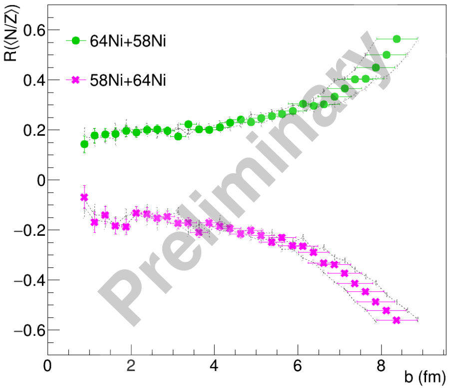

Isospin transport ratio: can highlight the isospin diffusion effect, bypassing the effects acting similarly on the four systems (F. Rami et al., Phys. Rev. Lett. 84, 1120 (2000))

$$R(x) = \frac{2x_i - x_{AA} - x_{BB}}{x_{AA} - x_{BB}}$$

$R(x) = \pm 1 \longrightarrow$ non equilibrated

$R(x_{AB}) = R(x_{BA}) \longrightarrow$ full equilibration

where $A = {}^{64}$Ni, $B = {}^{58}$Ni, $i = AA, AB, BA, BB$ and x is an isospin sensitive observable.

Model-independent isospin transport ratio R(⟨N/Z⟩) for the QP remnant as a function of the impact parameter b

Regular behavior towards equilibration for increasing centralities (full equilibration is not achieved).

Experimental result providing a reference for comparison with theoretical predictions from transport models.

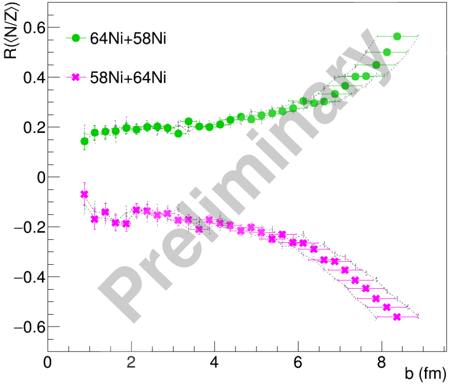

Isospin transport ratio: can highlight the isospin diffusion effect, bypassing the effects acting similarly on the four systems (F. Rami et al., Phys. Rev. Lett. 84, 1120 (2000))

$$R(x) = \frac{2x_i - x_{AA} - x_{BB}}{x_{AA} - x_{BB}}$$

$R(x) = \pm 1 \rightarrow$ non equilibrated

$R(x_{AB}) = R(x_{BA}) \rightarrow$ full equilibration

where $A = {}^{64}$Ni, $B = {}^{58}$Ni, $i = AA, AB, BA, BB$ and x is an isospin sensitive observable.

Model-independent isospin transport ratio R(⟨N/Z⟩) for the QP remnant as a function of the impact parameter b

Regular behavior towards equilibration for increasing centralities (full equilibration is not achieved).

Experimental result providing a reference for comparison with theoretical predictions from transport models.

The isospin transport ratio is also largely unaffected by statistical deexcitation.

A. Camaiani et al., Phys. Rev. C 102, 044607 (2020),
S. Mallik et al., J. Phys. G 49, 015102 (2021)

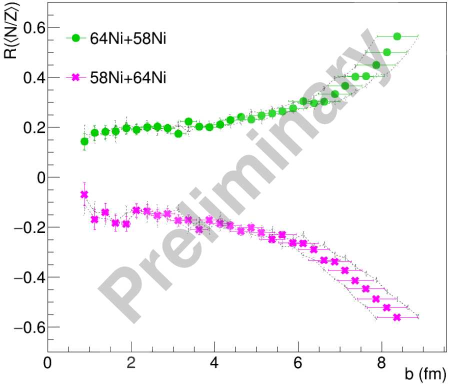

Preliminary comparison with theoretical predictions

BUU@VECC-McGill model predictions for different E_{sym}

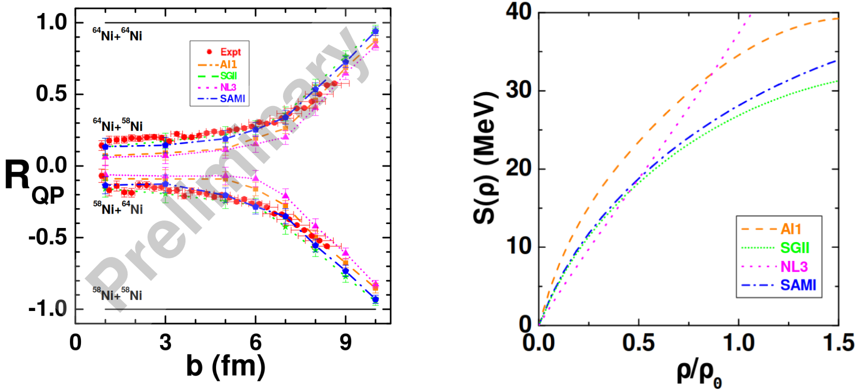

Comparison of experimental R(⟨N/Z⟩) vs b with theoretical predictions from BUU@VECC-McGill transport model for primary QP fragment.

No afterburner coupled to transport code (S. Mallik et al., J. Phys. G 49, 015102 (2021)).

Some differences arise among model predictions assuming different symmetry energy parametrizations, particularly for semicentral collisions. Multiple E_{sym} parametrizations are being explored (J. Margueron et al., Phys. Rev. C 97, 025806 (2018)).

Conclusions

Summary

- The assessment of the reaction centrality is crucial to exploit the experimental information as best as possible
- Application of impact parameter reconstruction method of J. D. Frankland et al., PRC104, 034609 (2021):
  - Combined analysis of two datasets (INDRA and INDRA-FAZIA) of Ni-Ni reactions at 32MeV/nucleon
  - *Experimental result:* isospin transport ratio calculated on the $\langle N/Z \rangle$ of QP remnant, studied as a function of a model-independent impact parameter
  - *Model predictions:* first comparisons with predictions for primary QP fragments from BUU@VECC-McGill transport model
- This model independent experimental assessment of the isospin diffusion effect across varying reaction centralities can represent a benchmark to test the performance of transport models and to gain further insight on the NEoS behavior for sub- to saturation densities

Thank you!

Backup slides

Impact parameter reconstruction

Detailed structure of the method

Given a centrality observable X, its inclusive distribution $P(X)$ can be expressed as:

$$P(X) = \int_0^{\infty} P(X,b)\,db = \int_0^{\infty} P(b)\,P(X|b)\,db = \int_0^{1} P(X|c_b)\,dc_b$$

where a change of variables is applied, introducing the centrality $c_b \equiv \int_0^b P(b')\,db'$ and exploiting that $P(c_b) = 1$.

Key step: model the $P(X|c_b)$ and extract its parameters by fitting the experimental $P(X)$

X assumes positive values $\longrightarrow$ non-negative gamma distribution as fluctuation kernel:

$$P(X|c_b) = \frac{1}{\Gamma(k)\theta^k}\,X^{k-1}\,e^{-X/\theta} \qquad \text{where } \bar{X} = k\theta \text{ and } \sigma_X = \sqrt{k}\theta$$

where k and θ generally evolve with centrality. For them we assume:

- $k(c_b) = k_{\max}[1 - c_b^{\alpha}]^{\gamma} + k_{\min}$, where α, γ, $k_{\min}$ and $k_{\max}$ are parameters of the fit
- θ independent of centrality (problem is underconstrained) $\longrightarrow$ θ is a fit parameter

Once the $P(X|c_b)$ is determined, one obtains:

$$P\left(c_b|x_1 \le X \le x_2\right) = \frac{\int_{x_1}^{x_2} P(c_b,X)\,dX}{\int_{x_1}^{x_2} P(X)\,dX} = \frac{\int_{x_1}^{x_2} P(X|c_b)\,dX}{\int_{x_1}^{x_2} P(X)\,dX}$$

and by changing back the variable: $P\left(b|x_1 \le X \le x_2\right) = P(b)\,P\left(c_b(b)|x_1 \le X \le x_2\right)$

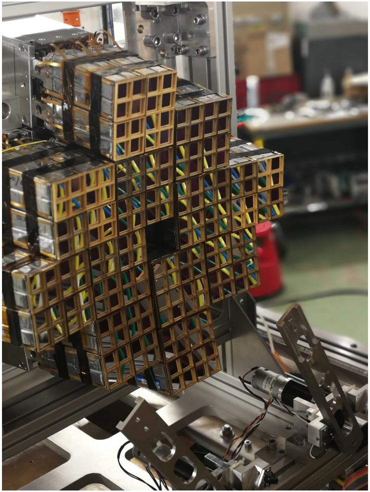

FAZIA *(Forward-angle A and Z Identification Array)*: optimal ion identification in the Fermi energy domain.

- Result of R&D activities to refine:
  - detector performance
  - digital treatment of signals
- Basic module: **block**, consisting of 16 three stage **telescopes** ($2 \times 2\,\text{cm}^2$ active area):
  - Si1 300 μm thick
  - Si2 500 μm thick
  - CsI(Tl) 10cm thick

  + read-out electronics for all telescopes.
- Identification techniques: ΔE-E / PSA
  - Charge discrimination tested up to $Z \sim 55$
  - Mass discrimination up to $Z \sim 25$ / $Z \sim 22$

R. Bougault et al., Eur. Phys. J. A 50, 47 (2014)
S. Valdré et al., NIMA 930, 27 (2019)

INDRA *(Identification de Noyaux et Détection avec Résolutions Accrues)*: highly segmented array for detection and identification of charged products of heavy ion collisions at intermediate energies ($10 < E < 100\, A$MeV).

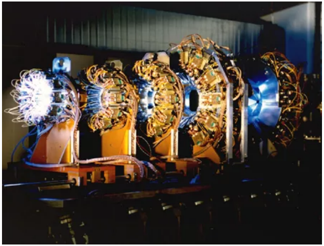

- Original configuration of 17 rings:
  - 1: Phoswich detectors
  - 2-9: Ionisation ch. + Si + CsI(Tl)
  - 10-17: Ionisation ch. + CsI(Tl)
- Charge discrimination up to uranium, mass discrimination up to $Z \sim 4$
  → Electronics upgrade (2020): now up to $Z \sim 10$
  J. D. Frankland et al., Nuovo Cim. C 45, 43 (2022)
- Large solid angle coverage (90%) with high granularity (336 modules)